ADI FINITE DIFFERENCE SCHEMES FOR OPTION PRICING IN THE HESTON MODEL WITH CORRELATION

K. J. IN 'T HOUT AND S. FOULON

Abstract. This paper deals with the numerical solution of the Heston partial differential equation (PDE) that plays an important role in financial option pricing theory, Heston (1993). A feature of this time-dependent, two-dimensional convection-diffusion-reaction equation is the presence of a mixed spatial-derivative term, which stems from the correlation between the two underlying stochastic processes for the asset price and its variance.

Semi-discretization of the Heston PDE, using finite difference schemes on non-uniform grids, gives rise to large systems of stiff ordinary differential equations. For the effective numerical solution of these systems, standard implicit time-stepping methods are often not suitable anymore, and tailored time-discretization methods are required. In the present paper, we investigate four splitting schemes of the Alternating Direction Implicit (ADI) type: the Douglas scheme, the Craig–Sneyd scheme, the Modified Craig–Sneyd scheme, and the Hundsdorfer–Verwer scheme, each of which contains a free parameter.

ADI schemes were not originally developed to deal with mixed spatial-derivative terms. Accordingly, we first discuss the adaptation of the above four ADI schemes to the Heston PDE. Subsequently, we present various numerical examples with realistic data sets from the literature, where we consider European call options as well as down-and-out barrier options. Combined with ample theoretical stability results for ADI schemes that have recently been obtained in In 't Hout & Welfert (2007, 2009) we arrive at three ADI schemes that all prove to be very effective in the numerical solution of the Heston PDE with a mixed derivative term. It is expected that these schemes will be useful also for general two-dimensional convection-diffusion-reaction equations with mixed derivative terms.

Key Words. Initial-boundary value problems, convection-diffusion equations, mixed derivatives, Heston model, option pricing, method-of-lines, finite difference methods, ADI splitting schemes.

1. Introduction

In the Heston model, values of options are given by a time-dependent partial differential equation (PDE) that is supplemented with initial and boundary conditions [7, 14, 22, 24]. The Heston PDE constitutes an important two-dimensional extension to the celebrated, one-dimensional, Black–Scholes PDE. Contrary to the

Black–Scholes model, however, to date in the Heston model no closed-form analytical formulas have been found for any but the simplest options, and therefore numerical techniques are applied.

A well-known and versatile strategy for the numerical solution of initial-boundary value problems for multi-dimensional PDEs is the method-of-lines approach. In this approach, the PDE is first discretized in the spatial variables, yielding large systems of stiff ordinary differential equations. These, so-called, semi-discrete systems are subsequently solved by applying a suitable numerical time-stepping method. Due to the large size and the multi-dimensional structure of the obtained semi-discrete systems, standard time-stepping methods, such as the popular Crank–Nicolson scheme (trapezoidal rule), are often not effective anymore, and tailored time discretization methods are required.

For the numerical solution of the semi-discrete Heston PDE we shall study in this paper splitting schemes of the Alternating Direction Implicit (ADI) type. In the past decades, ADI schemes have been successful already in many application areas. A main and distinctive feature of the Heston PDE, however, is the presence of a mixed spatial-derivative term, stemming from the correlation between the two underlying stochastic processes for the asset price and its variance. It is well-known that ADI schemes were not originally developed to deal with such terms. In the present paper, we will investigate the adaptation of several important ADI schemes to the numerical solution of the Heston PDE with arbitrary correlation factor $\rho \in [-1, 1]$. As test cases we will consider European call options and down-and-out barrier options. Through various numerical examples with realistic data sets from the literature, combined with ample theoretical stability results that have recently been obtained, we arrive at three ADI schemes that all prove to be very effective in the numerical solution of the Heston PDE with a mixed derivative term. It is expected that these schemes will be useful also for general two-dimensional convection-diffusion-reaction equations with mixed derivative terms.

An outline of our paper is as follows.

Section 2 discusses the Heston PDE and its numerical discretization. In Section 2.1 we formulate the Heston PDE together with initial and boundary conditions for European call options. In Section 2.2 we describe a finite difference discretization of the Heston PDE. A non-uniform spatial grid is used to capture the important region around the strike. In Section 2.3 we formulate the ADI type schemes under consideration in this paper for the semi-discrete Heston PDE with a mixed derivative term: the Douglas scheme, the Craig–Sneyd scheme, the Modified Craig–Sneyd scheme, and the Hundsdorfer–Verwer scheme. Each of these contains a free parameter θ. We discuss the different origins of the four schemes and review theoretical stability results that were recently obtained in [9, 10] concerning their application to multi-dimensional convection-diffusion equations with mixed derivative terms.

Section 3 contains extensive numerical experiments. In Section 3.1 we study the accuracy of our finite difference discretization in various examples of parameter sets for the Heston model obtained from the literature. Here the availability of Heston's analytical pricing formula for European call options makes an actual computation of the global spatial errors possible. In Section 3.2 we perform numerical experiments with all the ADI schemes above, where we analyze the behavior of the global temporal errors for each example introduced in Section 3.1. As an alternative method, we also consider a Runge–Kutta–Chebyshev scheme. In Section 3.3 we discuss numerical experiments for down-and-out call options. For these exotic

options a closed-form analytical pricing formula has only been obtained [14] in the literature if the correlation $\rho = 0$.

Section 4 summarizes our conclusions concerning the four ADI schemes in the numerical solution of the Heston PDE with a mixed derivative term. Subsequently, several issues for future research are discussed.

2. Numerical discretization of the Heston PDE

2.1. The Heston PDE. Let $u(s, v, t)$ denote the price of a European option if at time $T - t$ the underlying asset price equals s and its variance equals v, where T is the given maturity time of the option. Heston's stochastic volatility model implies [7, 14, 22] that u satisfies[1] the parabolic PDE

$$(2.1) \quad \frac{\partial u}{\partial t} = \tfrac{1}{2} s^2 v \frac{\partial^2 u}{\partial s^2} + \rho \sigma s v \frac{\partial^2 u}{\partial s \partial v} + \tfrac{1}{2} \sigma^2 v \frac{\partial^2 u}{\partial v^2} + (r_d - r_f) s \frac{\partial u}{\partial s} + \kappa(\eta - v) \frac{\partial u}{\partial v} - r_d u$$

for $0 \leq t \leq T$, $s > 0$, $v > 0$. The Heston PDE (2.1) can be viewed as a time-dependent convection-diffusion-reaction equation, on an unbounded two-dimensional spatial domain. The parameter $\kappa > 0$ is the mean-reversion rate, $\eta > 0$ is the long-term mean, $\sigma > 0$ is the volatility-of-variance, $\rho \in [-1, 1]$ is the correlation between the two underlying Brownian motions, and r_d, r_f denote the domestic and foreign interest rates, respectively. In this paper we always assume that $2\kappa\eta > \sigma^2$, which is known as the Feller condition.

For a European call option, the payoff yields the initial condition

$$(2.2) \quad u(s, v, 0) = \max(0, s - K)$$

where $K > 0$ is the given strike price of the option. Further, a boundary condition at $s = 0$ holds,

$$(2.3) \quad u(0, v, t) = 0 \quad (0 \leq t \leq T).$$

At the boundary $v = 0$ no condition is specified. From the assumption $2\kappa\eta > \sigma^2$ it follows that this is an outflow boundary.

As a preliminary step towards the numerical solution of the initial-boundary value problem for the Heston PDE, the spatial domain is restricted to a bounded set $[0, S] \times [0, V]$ with fixed values S, V chosen sufficiently large. The following additional conditions at $s = S$ and $v = V$ are imposed for a European call option, cf. [7, 27]:

$$(2.4) \quad \frac{\partial u}{\partial s}(S, v, t) = e^{-r_f t} \quad (0 \leq t \leq T),$$

$$(2.5) \quad u(s, V, t) = s e^{-r_f t} \quad (0 \leq t \leq T).$$

Clearly, the boundary conditions (2.3), (2.5) are of Dirichlet type, whereas (2.4) is of Neumann type. We take $S = 8K$ and $V = 5$. This yields a negligible modeling error with respect to (2.1)–(2.3) on the unbounded domain for a wide range of parameter values.

---

[1] We assume w.l.o.g. that the market price of volatility risk is equal to zero.

2.2. Space discretization: finite difference schemes. For the initial-boundary value problem (2.1)–(2.5) we perform a spatial discretization on a Cartesian grid by finite difference (FD) schemes. Here we apply non-uniform meshes in both the s- and v-directions such that relatively many mesh points lie in the neighborhood of $s = K$ and $v = 0$, respectively. The application of such non-uniform meshes greatly improves the accuracy of the FD discretization compared to using uniform meshes. This is related to the facts that the initial function (2.2) possesses a discontinuity in its first derivative at $s = K$ and that for $v \approx 0$ the Heston PDE is convection-dominated. It is also natural to have many grid points near the point $(s, v) = (K, 0)$ as in practice this is the region in the (s, v)-domain where one wishes to obtain option prices. The type of non-uniform meshes that we employ has recently been considered e.g. by Tavella & Randall [24] and Kluge [13].

We first define the mesh in the s-direction. Let integer $m_1 \geq 1$ and constant $c > 0$. Let equidistant points $\xi_0 < \xi_1 < \ldots < \xi_{m_1}$ be given by

$$\xi_i = \sinh^{-1}(-K/c) + i \cdot \Delta\xi \quad (0 \leq i \leq m_1)$$

with

$$\Delta\xi = \frac{1}{m_1} [\sinh^{-1}((S - K)/c) - \sinh^{-1}(-K/c)].$$

Then a non-uniform mesh $0 = s_0 < s_1 < \ldots < s_{m_1} = S$ is defined through the transformation

$$(2.6) \qquad s_i = K + c \sinh(\xi_i) \quad (0 \leq i \leq m_1).$$

This mesh is *smooth* in the sense that there exist real constants $C_0, C_1, C_2 > 0$ such that the mesh widths $\Delta s_i = s_i - s_{i-1}$ satisfy

$$(2.7) \qquad C_0 \, \Delta\xi \leq \Delta s_i \leq C_1 \, \Delta\xi \quad \text{and} \quad |\Delta s_{i+1} - \Delta s_i| \leq C_2 \, (\Delta\xi)^2$$

uniformly in i and m_1. The parameter c controls the fraction of mesh points s_i that lie in the neighborhood of the strike K. In particular,

$$\Delta s_i \approx c \, \Delta\xi \quad \text{whenever } s_i \approx K.$$

In our numerical experiments we have taken $c = K/5$.

We define a non-uniform mesh in the v-direction analogously. Let integer $m_2 \geq 1$ and constant $d > 0$. Consider equidistant points given by $\eta_j = j \cdot \Delta\eta$ for $j = 0, 1, \ldots, m_2$ with

$$\Delta\eta = \frac{1}{m_2} \sinh^{-1}(V/d).$$

Then we define a mesh $0 = v_0 < v_1 < \ldots < v_{m_2} = V$ through

$$(2.8) \qquad v_j = d \sinh(\eta_j) \quad (0 \leq j \leq m_2)$$

and write $\Delta v_j = v_j - v_{j-1}$. Also the mesh (2.8) is smooth. The parameter d controls the fraction of mesh points v_j that lie near $v = 0$. It holds that

$$\Delta v_j \approx d \, \Delta\eta \quad \text{whenever } v_j \approx 0.$$

In our experiments we have taken $d = V/500$.

As an illustration, Figure 1 displays the spatial grid defined by (2.6), (2.8) for the (small) sample values $m_1 = 30$, $m_2 = 15$ where $K = 100$. Clearly, there are many grid lines near $s = K$ and $v = 0$.

We subsequently formulate the FD schemes that we use. Let $f : \mathbb{R} \to \mathbb{R}$ be any given function, let $x_0 < x_1 < x_2 < \ldots < x_m$ be any given mesh points and $\Delta x_i = x_i - x_{i-1}$. To approximate the first derivative $f'(x_i)$, we consider three FD schemes:
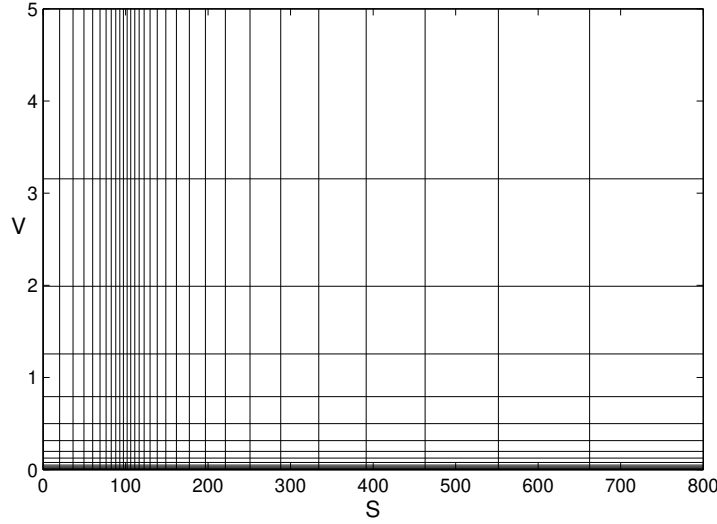
FIGURE 1. Sample grid defined by (2.6), (2.8) for $m_1 = 30$, $m_2 = 15$, $K = 100$.

$$(2.9a) \qquad f'(x_i) \; \approx \; \alpha_{i,-2}\, f(x_{i-2}) + \alpha_{i,-1}\, f(x_{i-1}) + \alpha_{i,0}\, f(x_i) \;,$$

$$(2.9b) \qquad f'(x_i) \; \approx \; \beta_{i,-1}\, f(x_{i-1}) + \beta_{i,0}\, f(x_i) + \beta_{i,1}\, f(x_{i+1}) \;,$$

$$(2.9c) \qquad f'(x_i) \; \approx \; \gamma_{i,0}\, f(x_i) + \gamma_{i,1}\, f(x_{i+1}) + \gamma_{i,2}\, f(x_{i+2}) \;,$$

with coefficients given by

$$\alpha_{i,-2} = \frac{\Delta x_i}{\Delta x_{i-1}(\Delta x_{i-1}+\Delta x_i)} \;,\; \alpha_{i,-1} = \frac{-\Delta x_{i-1}-\Delta x_i}{\Delta x_{i-1}\Delta x_i} \;,\; \alpha_{i,0} = \frac{\Delta x_{i-1}+2\Delta x_i}{\Delta x_i(\Delta x_{i-1}+\Delta x_i)} \;,$$

$$\beta_{i,-1} = \frac{-\Delta x_{i+1}}{\Delta x_i(\Delta x_i+\Delta x_{i+1})} \;,\; \beta_{i,0} = \frac{\Delta x_{i+1}-\Delta x_i}{\Delta x_i\Delta x_{i+1}} \;,\; \beta_{i,1} = \frac{\Delta x_i}{\Delta x_{i+1}(\Delta x_i+\Delta x_{i+1})} \;,$$

$$\gamma_{i,0} = \frac{-2\Delta x_{i+1}-\Delta x_{i+2}}{\Delta x_{i+1}(\Delta x_{i+1}+\Delta x_{i+2})} \;,\; \gamma_{i,1} = \frac{\Delta x_{i+1}+\Delta x_{i+2}}{\Delta x_{i+1}\Delta x_{i+2}} \;,\; \gamma_{i,2} = \frac{-\Delta x_{i+1}}{\Delta x_{i+2}(\Delta x_{i+1}+\Delta x_{i+2})} \;.$$

To approximate the second derivative $f''(x_i)$, we deal with the FD scheme

$$(2.10) \qquad f''(x_i) \; \approx \; \delta_{i,-1}\, f(x_{i-1}) + \delta_{i,0}\, f(x_i) + \delta_{i,1}\, f(x_{i+1}) \;,$$

where

$$\delta_{i,-1} = \frac{2}{\Delta x_i(\Delta x_i+\Delta x_{i+1})} \;,\; \delta_{i,0} = \frac{-2}{\Delta x_i\Delta x_{i+1}} \;,\; \delta_{i,1} = \frac{2}{\Delta x_{i+1}(\Delta x_i+\Delta x_{i+1})} \;.$$

Next, assume $f : \mathbb{R}^2 \to \mathbb{R}$ is a function of two variables (x,y). We consider approximating the mixed derivative $f_{xy}(x,y)$. Let x_i, Δx_i be as above, let mesh points $y_0 < y_1 < y_2 < \ldots < y_n$ in the y-direction be given, and write $\Delta y_j = y_j - y_{j-1}$. Denote by $\hat{\beta}_{i,k}$ the coefficients analogous to $\beta_{i,k}$ in (2.9b), but then relevant to the y-direction. For the discretization of the mixed derivative we use the FD scheme

$$(2.11) \qquad \frac{\partial^2 f}{\partial x \partial y}(x_i, y_j) \; \approx \; \sum_{k,\, l=-1}^{1} \beta_{i,k}\, \hat{\beta}_{j,l}\, f(x_{i+k}, y_{j+l}) \;.$$

Clearly, the approximation (2.11) can be viewed as obtained by application of (2.9b) successively in the x- and y-directions.

The FD schemes above are all well-known. Formulas (2.9b), (2.10), (2.11) are *central* schemes, whereas (2.9a), (2.9c) are *upwind* schemes. We note that these schemes have previously been applied by Kluge [13] in the numerical solution of the Heston PDE. Through Taylor expansion it can be verified that each of the formulas (2.9), (2.10), (2.11) has a second-order truncation error, provided that the function f is sufficiently often continuously differentiable and the meshes in the x- and y-directions are smooth, cf. (2.7).

The actual FD discretization of the initial-boundary value problem for the Heston PDE is performed as follows.

In view of the Dirichlet boundary conditions (2.3) and (2.5), the grid in $[0, S] \times [0, V]$ is given by

$$G = \{(s_i, v_j) : 1 \le i \le m_1, \ 0 \le j \le m_2 - 1\}.$$

At this grid, each spatial derivative appearing in (2.1) is replaced by its corresponding central FD scheme (2.9b), (2.10), or (2.11) – except in the region $v > 1$ and at the boundaries $v = 0$ and $s = S$.

In the region $v > 1$ we apply the upwind scheme (2.9a) for $\partial u / \partial v$ whenever the flow in the v-direction is towards $v = V$. This is done so as to avoid spurious oscillations in the FD solution when the volatility-of-variance σ is close to zero.

At the outflow boundary $v = 0$ the derivative $\partial u / \partial v$ is approximated using the upwind scheme (2.9c). All other derivative terms in the v-direction vanish at $v = 0$, due to the factor v occurring in (2.1), and hence, these terms do not require further treatment.

At the boundary $s = S$ the spatial derivatives in the s-direction need to be considered. First, the Neumann condition (2.4) at $s = S$ implies that the mixed derivative $\partial^2 u / \partial s \partial v$ vanishes there. Next, the derivative $\partial u / \partial s$ is directly given by (2.4). Finally, we approximate $\partial^2 u / \partial s^2$ at $s = S = s_{m_1}$ using the central scheme (2.10) with the virtual point $S + \Delta s_{m_1}$, where the value at this point is defined by extrapolation using (2.4).

The FD discretization described above of the initial-boundary value problem (2.1)–(2.5) for the Heston PDE yields an initial value problem for a large system of stiff ordinary differential equations (ODEs),

$$(2.12) \qquad U'(t) = AU(t) + b(t) \quad (0 \le t \le T), \quad U(0) = U_0.$$

Here A is a given $m \times m$–matrix and $b(t)$ $(t \ge 0)$, U_0 are given m–vectors with $m = m_1 m_2$. The vector U_0 is directly obtained from the initial condition (2.2) and the vector function b depends on the boundary conditions (2.3)–(2.5). For each given $t > 0$, the entries of the solution vector $U(t)$ to (2.12) constitute approximations to the exact solution values $u(s, v, t)$ of (2.1)–(2.5) at the spatial grid points $(s, v) \in G$, ordered in a convenient way.

2.3. Time discretization: ADI schemes.
Acquiring an effective numerical time-discretization method for the spatially discretized Heston problem (2.12) is a key step in arriving at a full numerical solution scheme for the Heston PDE that is both efficient and robust.

Let $\Delta t > 0$ be a given time step and let temporal grid points be given by $t_n = n\Delta t$ for $n = 0, 1, 2, \dots$. A well-known method for the numerical solution of stiff initial value problems for systems of ODEs

$$(2.13) \qquad U'(t) = F(t, U(t)) \quad (0 \le t \le T), \quad U(0) = U_0$$

is the *Crank–Nicolson scheme* or *trapezoidal rule*. This method defines approximations U_n to the exact solution values $U(t_n)$ of (2.13) successively for $n = 1, 2, 3, \ldots$ by

$$(2.14) \qquad U_n = U_{n-1} + \tfrac{1}{2}\Delta t F(t_{n-1}, U_{n-1}) + \tfrac{1}{2}\Delta t F(t_n, U_n).$$

In our case of (2.12) we have

$$(2.15) \qquad F(t, w) = Aw + b(t) \quad \text{for } 0 \le t \le T, \ w \in \mathbb{R}^m.$$

Thus, each step (2.14) requires the solution of a system of linear equations involving the matrix $(I - \tfrac{1}{2}\Delta t A)$ where I denotes the $m \times m$ identity matrix. Since $(I - \tfrac{1}{2}\Delta t A)$ does not depend on the step index n, one can compute a LU factorization of this matrix once, beforehand, and next apply it in all steps (2.14) to obtain U_n $(n \ge 1)$.

The Crank–Nicolson scheme can be practical when the number of spatial grid points $m = m_1 m_2$ is moderate. In our application to the two-dimensional Heston PDE, however, m usually gets large and the Crank–Nicolson scheme becomes ineffective. The reason for this is that $(I - \tfrac{1}{2}\Delta t A)$, and hence the matrices in its LU factorization, possess a bandwidth that is directly proportional to $\min\{m_1, m_2\}$.

For the numerical solution of the semi-discretized Heston problem (2.12) we shall consider in this paper splitting schemes of the ADI type. We decompose the matrix A into three submatrices,

$$A = A_0 + A_1 + A_2.$$

We choose the matrix A_0 as the part of A that stems from the FD discretization of the mixed derivative term in (2.1). Next, in line with the classical ADI idea, we choose A_1 and A_2 as the two parts of A that correspond to all spatial derivatives in the s- and v-directions, respectively. The $r_d u$ term in (2.1) is distributed evenly over A_1, A_2. The FD discretization described in Sect. 2.2 implies that A_1, A_2 are essentially tridiagonal and pentadiagonal, respectively.

Write $b(t)$ from (2.12) as $b(t) = b_0(t) + b_1(t) + b_2(t)$ where the decomposition is analogous to that of A. Next, define functions F_j $(j = 0, 1, 2)$ by

$$(2.16) \qquad F_j(t, w) = A_j w + b_j(t) \quad \text{for } 0 \le t \le T, \ w \in \mathbb{R}^m.$$

Then for F given by (2.15) we have the splitting $F = F_0 + F_1 + F_2$. Clearly, $F_0 \ne 0$ whenever the correlation factor $\rho \ne 0$.

Let θ be a given real parameter. In the following we formulate four splitting schemes for the initial value problem (2.13). Here we assume that F stems from a FD discretization of a general 2D convection-diffusion equation with a mixed derivative term that is decomposed similarly as above for the semi-discrete Heston PDE. All four schemes generate, in a one-step manner, approximations U_n to the exact solution values $U(t_n)$ of (2.13) successively for $n = 1, 2, 3, \ldots$:

Douglas (Do) scheme:

$$(2.17) \qquad \begin{cases} Y_0 = U_{n-1} + \Delta t F(t_{n-1}, U_{n-1}), \\[2mm] Y_j = Y_{j-1} + \theta \Delta t \left(F_j(t_n, Y_j) - F_j(t_{n-1}, U_{n-1}) \right) \ (j = 1, 2), \\[2mm] U_n = Y_2 \end{cases}$$

Craig–Sneyd (CS) scheme:

$$(2.18) \quad \begin{cases} Y_0 = U_{n-1} + \Delta t F(t_{n-1}, U_{n-1}), \\[2mm] Y_j = Y_{j-1} + \theta \Delta t \left(F_j(t_n, Y_j) - F_j(t_{n-1}, U_{n-1}) \right) \ (j = 1, 2), \\[2mm] \widetilde{Y}_0 = Y_0 + \tfrac{1}{2} \Delta t \left(F_0(t_n, Y_2) - F_0(t_{n-1}, U_{n-1}) \right), \\[2mm] \widetilde{Y}_j = \widetilde{Y}_{j-1} + \theta \Delta t \left(F_j(t_n, \widetilde{Y}_j) - F_j(t_{n-1}, U_{n-1}) \right) \ (j = 1, 2), \\[2mm] U_n = \widetilde{Y}_2 \end{cases}$$

Modified Craig–Sneyd (MCS) scheme:

$$(2.19) \quad \begin{cases} Y_0 = U_{n-1} + \Delta t F(t_{n-1}, U_{n-1}), \\[2mm] Y_j = Y_{j-1} + \theta \Delta t \left(F_j(t_n, Y_j) - F_j(t_{n-1}, U_{n-1}) \right) \ (j = 1, 2), \\[2mm] \widehat{Y}_0 = Y_0 + \theta \Delta t \left(F_0(t_n, Y_2) - F_0(t_{n-1}, U_{n-1}) \right), \\[2mm] \widetilde{Y}_0 = \widehat{Y}_0 + (\tfrac{1}{2} - \theta) \Delta t \left(F(t_n, Y_2) - F(t_{n-1}, U_{n-1}) \right), \\[2mm] \widetilde{Y}_j = \widetilde{Y}_{j-1} + \theta \Delta t \left(F_j(t_n, \widetilde{Y}_j) - F_j(t_{n-1}, U_{n-1}) \right) \ (j = 1, 2), \\[2mm] U_n = \widetilde{Y}_2 \end{cases}$$

Hundsdorfer–Verwer (HV) scheme:

$$(2.20) \quad \begin{cases} Y_0 = U_{n-1} + \Delta t F(t_{n-1}, U_{n-1}), \\[2mm] Y_j = Y_{j-1} + \theta \Delta t \left(F_j(t_n, Y_j) - F_j(t_{n-1}, U_{n-1}) \right) \ (j = 1, 2), \\[2mm] \widetilde{Y}_0 = Y_0 + \tfrac{1}{2} \Delta t \left(F(t_n, Y_2) - F(t_{n-1}, U_{n-1}) \right), \\[2mm] \widetilde{Y}_j = \widetilde{Y}_{j-1} + \theta \Delta t \left(F_j(t_n, \widetilde{Y}_j) - F_j(t_n, Y_2) \right) \ (j = 1, 2), \\[2mm] U_n = \widetilde{Y}_2. \end{cases}$$

In the Do scheme (2.17), a forward Euler predictor step is followed by two implicit but unidirectional corrector steps, whose purpose is to stabilize the predictor step. The CS scheme (2.18), the MCS scheme (2.19) and the HV scheme (2.20) can be viewed as different extensions to the Do scheme. They all perform a second predictor step, followed by two unidirectional corrector steps.

Each of the above splitting schemes treats the mixed derivative part F_0 in a fully *explicit* way. Note that in the special case where $F_0 = 0$, the CS scheme reduces to the Do scheme, but the MCS scheme (with $\theta \neq \tfrac{1}{2}$) and the HV scheme do not.

The F_1 and F_2 parts are treated *implicitly* in all four schemes. In every step of each scheme, systems of linear equations need to be solved involving the two matrices $(I - \theta \Delta t A_j)$ for $j = 1, 2$. Like for the Crank–Nicolson scheme, these matrices do not depend on the step index n, and thus one can determine their LU factorizations once, beforehand, and next apply them in all time steps to compute U_n $(n \geq 1)$. However, the bandwidths of the matrices given by LU factorization

of $(I - \theta \Delta t A_j)$ $(j = 1, 2)$ are now *fixed*, i.e., independent of m_1 and m_2. As a consequence, in each of the four splitting schemes, the number of floating point operations per time step is directly proportional to m, which yields a big reduction compared to the Crank–Nicolson scheme.

For any parameter θ, the classical order of consistency of the Do scheme – for general F_0, F_1, F_2 – is just *one*. An advantage of the CS, MCS and HV schemes is that they can attain order of consistency *two* for general F_0, F_1, F_2. Taylor expansion shows that the CS scheme has order two if and only if $\theta = \frac{1}{2}$. Subsequently, the MCS and HV schemes have order two for any given θ. With the latter two schemes, the parameter θ can thus be chosen to meet additional requirements. A virtue of all four splitting schemes is that all internal vectors Y_j, $\widetilde{Y}_j$ form consistent approximations to $U(t_n)$.

The Do scheme can be regarded as a direct generalization of the classical ADI schemes for 2D diffusion equations by Douglas & Rachford [5] and Peaceman & Rachford [17] to the situation where a mixed spatial derivative term is present in the equation. This generalization was considered by McKee & Mitchell [15] for diffusion equations and then by McKee et. al. [16] for convection-diffusion equations.

The CS scheme was developed by Craig & Sneyd [4] with the aim to arrive at a stable *second-order* ADI scheme for diffusion equations with mixed derivative terms.

The MCS scheme has recently been introduced by In 't Hout & Welfert [10] to obtain more freedom in the choice of θ as compared to the second-order CS scheme.

The HV scheme was designed by Hundsdorfer [11] and Verwer et. al. [26] for the numerical solution of convection-diffusion-reaction equations arising in atmospheric chemistry, cf. also [12]. The application of the HV scheme to equations containing mixed derivative terms has recently been studied by In 't Hout & Welfert [9, 10].

Our formulation of the ADI schemes (2.17)–(2.20) is similar to the type of formulation used in [11]. In the literature, these schemes are also sometimes referred to as Stabilizing Correction schemes, and are further closely related to Approximate Matrix Factorization methods and IMEX methods, cf. e.g. [12].

ADI schemes have already been applied by various researchers for the numerical solution of PDE models in finance. Lipton [14] describes an ADI scheme for 2D convection-diffusion equations with a mixed derivative term that is closely related to the Do scheme with $\theta = \frac{1}{2}$. Andreasen [2] uses the Do scheme with $\theta = \frac{1}{2}$ for certain interest rate models without a mixed derivative term. Randall [19] applies the CS scheme with $\theta = \frac{1}{2}$ to the Heston PDE with a mixed derivative term. We note that actual numerical results were not reported in loc. cit. The HV scheme has recently been considered for the application to PDE models in finance by In 't Hout [8], where an initial experiment in the case of the Heston PDE with a mixed derivative term is discussed. As a corollary of our present paper we will find that the choice of $\theta = 0.3$ for the HV scheme [8] is not optimal with respect to robustness.

Theoretical stability results for all four ADI schemes – relevant to FD discretizations of 2D convection-diffusion equations with a mixed derivative term – have been derived in [4, 9, 10, 15, 16]. These results concern *unconditional* stability, i.e., without any restriction on the time step Δt. The analysis in loc. cit. has been performed following the classical von Neumann method (Fourier transformation), where the usual assumptions are made that the coefficients are constant, the boundary condition is periodic, the spatial grid is uniform, and stability is considered in the l_2-norm.

Currently, the most comprehensive stability results for the Do, CS, MCS and HV schemes relevant to multi-dimensional PDEs with mixed derivative terms have been obtained in [9, 10]. We review the main conclusions from loc. cit. relevant to the situation of our paper.

The Do and CS schemes are both unconditionally stable when applied to 2D convection-diffusion equations with a mixed derivative term whenever $\theta \geq \frac{1}{2}$. In particular, the second-order CS scheme is unconditionally stable.

The MCS and HV schemes are unconditionally stable when applied to 2D pure diffusion equations with a mixed derivative term whenever $\theta \geq \frac{1}{3}$ and $\theta \geq 1 - \frac{1}{2}\sqrt{2}$, respectively. Recall that the MCS and HV schemes are of order two for any given θ. At this moment, unconditional stability results for the MCS and HV schemes in the general situation of 2D equations, with convection, are lacking. It was conjectured [9] however that the HV scheme is unconditionally stable when applied to 2D convection-diffusion equations with a mixed derivative term whenever $\theta \geq \frac{1}{2} + \frac{1}{6}\sqrt{3}$.

3. Numerical experiments

3.1. Spatial discretization error. In this section we consider four numerical examples and assess the actual convergence behavior of the FD discretization (2.12) of the Heston PDE defined in Sect. 2.2. For any given numbers of mesh points m_1, m_2 in the s- and v-directions, we define the *global spatial discretization error* at time $t = T$ by

$$e(m_1, m_2) = \max \left\{ |u(s_i, v_j, T) - U_k(T)| : \ \tfrac{1}{2}K < s_i < \tfrac{3}{2}K, \ 0 < v_j < 1 \right\}.$$

Here u denotes the exact European call option price function, satisfying the initial-boundary value problem (2.1)–(2.3) for the Heston PDE on the unbounded domain. Next, U_k designates the component of the exact solution U to (2.12) that corresponds to the grid point (s_i, v_j).

Clearly, the global spatial error is defined via a maximum norm. The set of asset prices $s \in (\frac{1}{2}K, \frac{3}{2}K)$ and variances $v \in (0, 1)$ in our definition encompasses most situations of practical interest. We note that the modeling error, that was introduced by restricting the domain of the Heston PDE to a bounded set, is also contained in $e(m_1, m_2)$. In our experiments this contribution turns out to be negligible.

For the actual computation of the global spatial errors $e(m_1, m_2)$ we apply the HV scheme with $\theta = \frac{1}{2} + \frac{1}{6}\sqrt{3}$ to (2.12) with the small time step $\Delta t = T/1000$ to obtain a sufficiently accurate approximation of $U(T)$. Subsequently, we employ an implementation of Heston's semi-analytical formula [7] to acquire values of u. For calculating the single integrals occurring in this formula we use a numerical quadrature rule. Numerical difficulties one can encounter in the implementation, due to the presence of multi-valued complex functions, have recently been discussed in [1]. We adopt the algorithm proposed in loc. cit. where branch cuts in the complex plane are correctly taken into account.

We perform numerical experiments in the four cases of parameter sets given by Table 1. Observe that in three of the four cases there is a substantial correlation factor ρ. Only in case 4 the correlation factor is relatively small.

Case 1 has been taken from Albrecher et. al. [1], where we have chosen $T = 1$. Case 2 comes from Bloomberg [3]. A special feature of this parameter set is that σ is close to zero, which implies that the Heston PDE is convection-dominated in the v-direction. Values for r_d, r_f and T were not specified in [3] and have been

	Case 1	Case 2	Case 3	Case 4
κ	1.5	3	0.6067	2.5
η	0.04	0.12	0.0707	0.06
σ	0.3	0.04	0.2928	0.5
ρ	-0.9	0.6	-0.7571	-0.1
r_d	0.025	0.01	0.03	0.0507
r_f	0	0.04	0	0.0469
T	1	1	3	0.25
K	100	100	100	100

TABLE 1. Parameters for the Heston model and European call options.
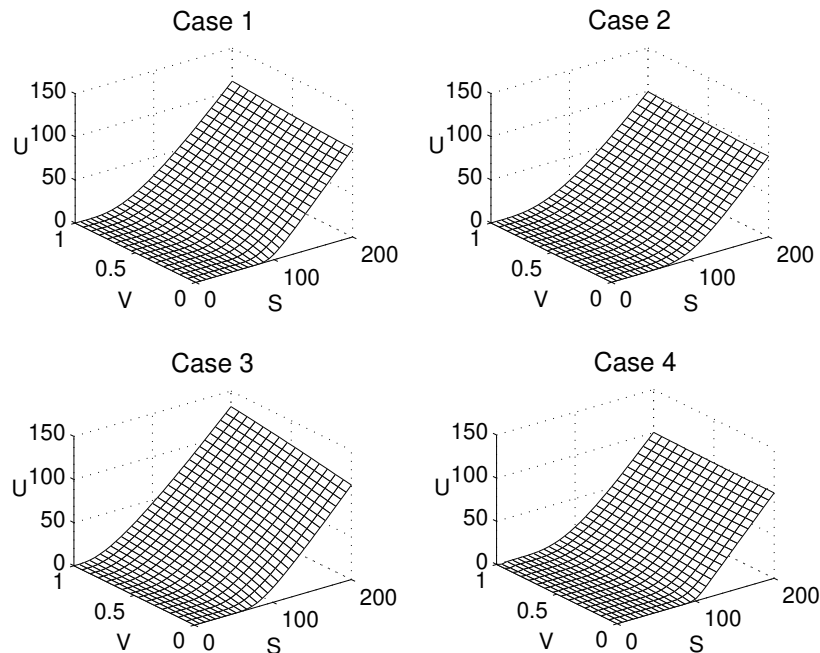
FIGURE 2. European call option price functions u in the four cases given by Table 1.

chosen separately. Case 3 has been taken from Schoutens et. al. [21]. Here the Feller condition is only just met. Finally, case 4 stems from Winkler et. al. [27].

Figure 2 displays the exact option price functions u corresponding to the four cases of Table 1 on the domain $(s, v) \in [0, 200] \times [0, 1]$.

Figure 3 subsequently shows for each case from Table 1 the global spatial errors $e(2m_2, m_2)$ vs. $1/m_2$ for $m_2 = 10, 20, \ldots, 100$. We have taken $m_1 = 2m_2$ as it turns out that, for efficiency reasons, one can use much less points in the v-direction than in the s-direction. To determine the numerical order of convergence p of the spatial discretization, we have fitted in each case a straight line to the outcomes for the global spatial errors. Accordingly, in the cases 1, 2, 3, 4 we found the respective
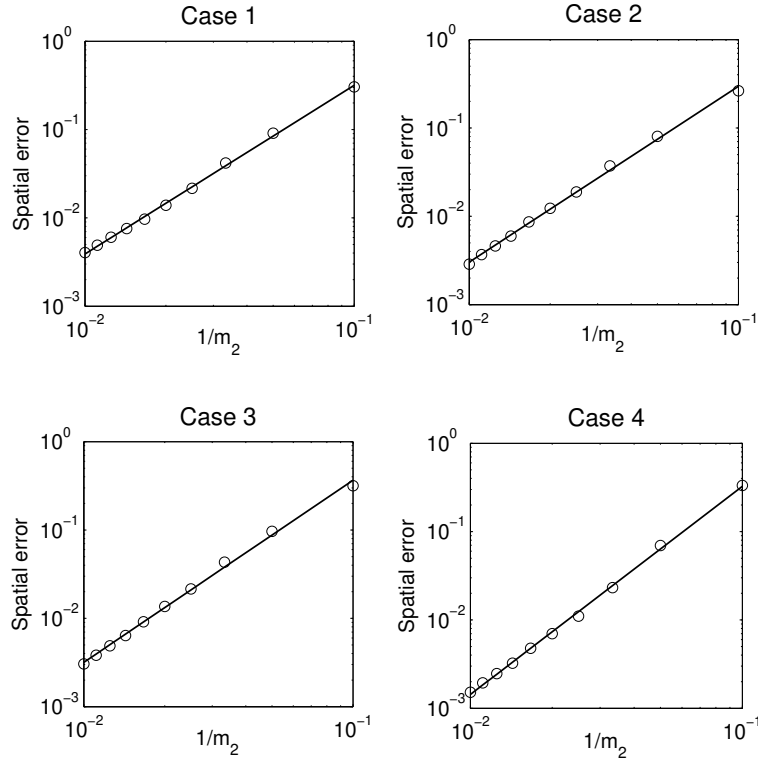
FIGURE 3. Global spatial errors $e(2m_2, m_2)$ vs. $1/m_2$ for $m_2 = 10, 20, \ldots, 100$ in the four cases given by Table 1 with least-squares fit superimposed.

orders $p = 1.9$, 2.0, 2.1, 2.4. This clearly suggests that the FD discretization of the Heston PDE described in Sect. 2.2 is convergent of appr. order two.

We remark that for the global spatial errors in relative sense, we obtained in each case that it is close to 1.0 percent for $m_2 = 30$ and decreases to approximately 0.1 percent for $m_2 = 100$. Here asset-variance pairs (s_i, v_j) are considered such that the option value $u(s_i, v_j, T)$ is always at least 1.

Finally, we repeated the numerical experiments above for uniform grids. Then the global spatial errors are always found to be much larger, compared to the non-uniform grid under consideration with the same number of points. Furthermore, the error behavior is erratic in this case. The latter can be seen to be related to the relative position of the point $s = K$ to the mesh in the s-direction, and concerns a known phenomenon, see e.g. Tavella & Randall [24]. This behavior is much less noticeable for (suitable) non-uniform grids.

3.2. Temporal discretization error. In this section we present numerical experiments for the ADI schemes (2.17), (2.18), (2.19), (2.20) which yields important insight into their actual stability and convergence behavior in the application to semi-discretized Heston problems (2.12) with non-zero correlation.

We define the *global temporal discretization error* at time $t = T = N\Delta t$ by

$$\widehat{e}(N; m_1, m_2) = \max\left\{ |U_k(T) - U_{N,k}| : \tfrac{1}{2}K < s_i < \tfrac{3}{2}K, \ 0 < v_j < 1 \right\},$$
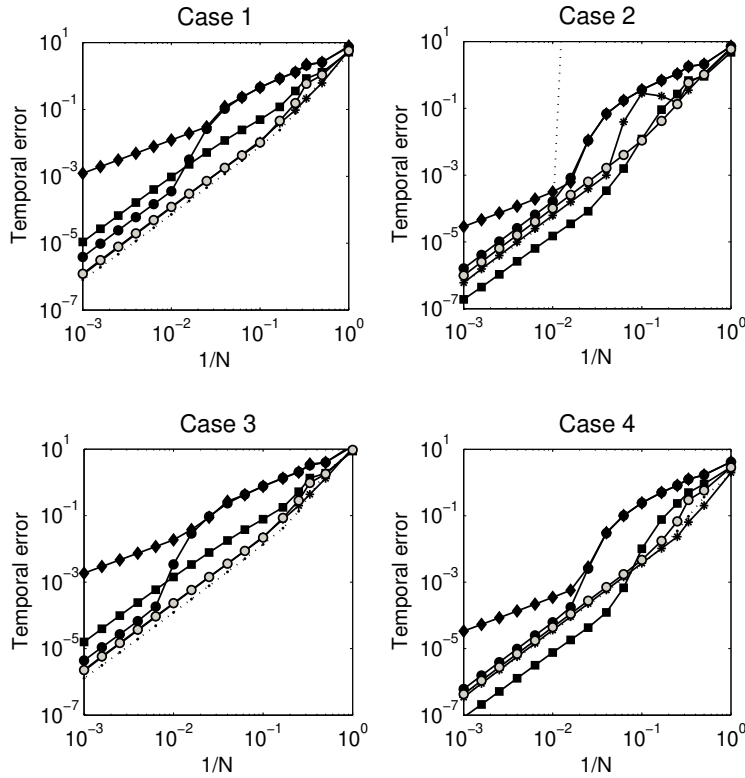
FIGURE 4. Global temporal errors $\widehat{e}(N; 100, 50)$ vs. $1/N$ in the four cases given by Table 1. Schemes: RKC with $\varepsilon = 10$ (dotted line), Do with $\theta = \frac{1}{2}$ (diamond), CS with $\theta = \frac{1}{2}$ (circle), MCS with $\theta = \frac{1}{3}$ (grey circle), HV with $\theta = 1 - \frac{1}{2}\sqrt{2}$ (star) and HV with $\theta = \frac{1}{2} + \frac{1}{6}\sqrt{3}$ (square).

where the index k is such that $U_k(T)$ and $U_{N,k}$ correspond to the spatial grid point (s_i, v_j). Clearly, the global temporal error is defined for the same (s, v)-domain as the global spatial error and we also deal again with the maximum norm, cf. Sect. 3.1.

Motivated by the theoretical stability and accuracy results discussed in Sect. 2.3, we shall consider the Do and CS schemes with $\theta = \frac{1}{2}$ and the MCS scheme with $\theta = \frac{1}{3}$. Next, we consider the HV scheme for the two values $\theta = 1 - \frac{1}{2}\sqrt{2} \approx 0.293$ and $\theta = \frac{1}{2} + \frac{1}{6}\sqrt{3} \approx 0.789$, to which we refer in the following as HV1 and HV2, respectively. We apply all these ADI schemes in each of the four cases of parameter sets for European call options in the Heston model listed in Table 1.

In addition, we also apply the Runge–Kutta–Chebyshev (RKC) scheme. This is an explicit second-order Runge–Kutta scheme which has been constructed such that its stability region includes a large interval $[-\beta, 0]$ along the negative real axis. For a complete discussion of this method see e.g. [12, 23]. The RKC scheme has a free parameter ε. Since the Heston PDE contains a convective part, we have chosen $\varepsilon = 10$, cf. [25]. In this case $\beta \approx 0.34(\nu^2 - 1)$, where ν denotes the number of stages of the scheme. Accordingly, in a given application to a semi-discretized Heston
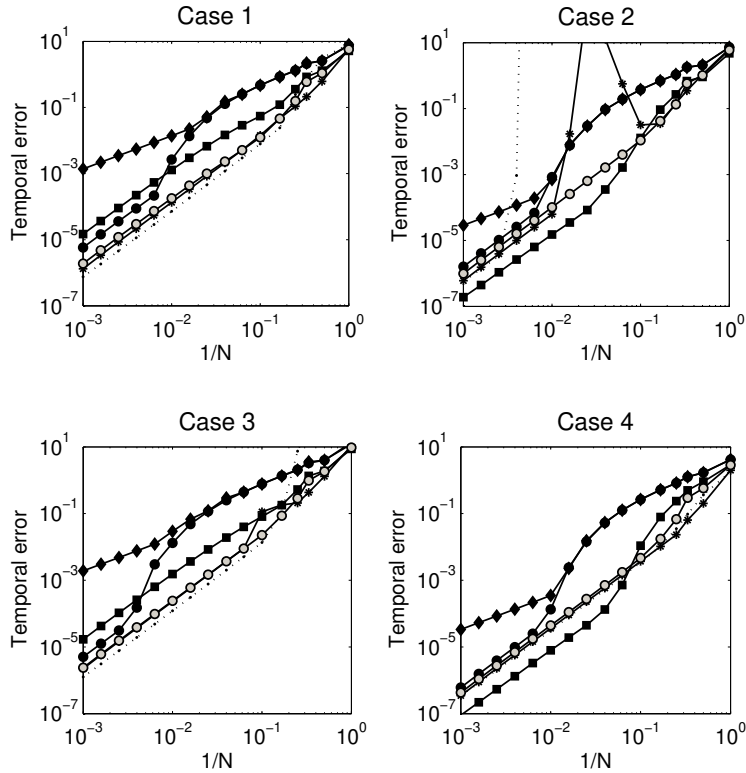
FIGURE 5. Global temporal errors $\widehat{e}(N; 200, 100)$ vs. $1/N$ in the four cases given by Table 1. Schemes: RKC with $\varepsilon = 10$ (dotted line), Do with $\theta = \frac{1}{2}$ (diamond), CS with $\theta = \frac{1}{2}$ (circle), MCS with $\theta = \frac{1}{3}$ (grey circle), HV with $\theta = 1 - \frac{1}{2}\sqrt{2}$ (star) and HV with $\theta = \frac{1}{2} + \frac{1}{6}\sqrt{3}$ (square).

problem (2.12) with time step Δt, the number of stages is taken as the smallest integer $\nu \geq \sqrt{1 + 3\Delta t\, r[A]}$ where $r[A]$ denotes the spectral radius of A.

Figures 4, 5 display for $m_1 = 2m_2 = 100$ and $m_1 = 2m_2 = 200$, respectively, the results for the global temporal errors $\widehat{e}(N; m_1, m_2)$ vs. $1/N$ for a range of step numbers N between $N = 1$ and $N = 1000$. We applied the HV2 scheme with $N = 5000$ to obtain a reference value for $U(T)$.

A first observation from Figures 4, 5 is that in the cases 1, 3, 4 the RKC scheme has global temporal errors that are often comparable to those of the MCS scheme. For relatively large Δt, however, the RKC scheme requires a large number of stages ν since in all cases $r[A] \approx 5.1 \cdot 10^4$ (if $m_1 = 2m_2 = 100$) and $r[A] \approx 2.2 \cdot 10^5$ (if $m_1 = 2m_2 = 200$). In our experiments, RKC always turned out to be considerably less efficient than MCS. Note that because the RKC scheme does produce fair temporal errors for all N in each of the cases 1, 3, 4, this suggests that the eigenvalues of the corresponding matrices A all lie close to the negative real axis in these three cases. In case 2, the RKC scheme clearly shows instability for, at least, values $N < 100$. We explain this from the corresponding matrices A to have eigenvalues

in the left half of the complex plane with substantial imaginary parts. This is also conceivable, since in case 2 the Heston PDE is convection-dominated in the v-direction, cf. Sect. 3.1.

For the Do, CS, MCS and HV2 schemes, the Figures 4, 5 clearly reveal that in all cases 1–4 the global temporal errors always stay below a moderate bound and decrease monotonically with N. This is a very favorable result and indicates an unconditionally stable behavior of these ADI schemes in all cases. Note that it is a non-trivial result, as it does not directly follow e.g. from the von Neumann analysis discussed in Sect. 2.3.

For the HV1 scheme, case 2 shows a peak in the global temporal errors which is higher if $m_1 = 2m_2 = 200$ than if $m_1 = 2m_2 = 100$. We conjecture that the HV1 scheme is just conditionally stable, under a CFL condition. We mention in passing that the same is found for the HV scheme with value $\theta = 0.3$, cf. [8].

Subsequent analysis of the results in Figures 4, 5 yields for the MCS and HV2 schemes in each case 1–4 a convergence order equal to 2.0. Moreover, the convergence behavior is of the form $C(\Delta t)^2$ $(0 < \Delta t \leq \tau)$ with constants C, $\tau > 0$ that are only weakly dependent on the number of spatial grid points m. Hence, the MCS and HV2 schemes show a stiff order of convergence equal to two. This clearly agrees with their orders of consistency, cf. Sect. 2.3. Remark that this is not obvious, as the order of consistency is a priori only relevant to fixed, non-stiff ODEs.

For the HV1 scheme, we obtain a stiff order of convergence equal to two in the cases 1, 3, 4.

The Do and CS schemes exhibit in all cases an undesirable convergence behavior, with temporal errors that are relatively large for modest time steps Δt. This atypical behavior becomes more pronounced when m_1, m_2 get larger. Though the results are not included in the figures, we remark that the (time-consuming) Crank–Nicolson scheme shows a similar behavior. The cause for this phenomenon is related to the fact that at $s = K$ the payoff function (2.2) is non-smooth and the Do, CS and Crank–Nicolson schemes do not sufficiently damp local (high-frequency) errors incited by this. A remedy for this situation is to first apply, at $t = 0$, two backward Euler steps with step size $\Delta t/2$, and then to proceed onwards from $t = \Delta t$ with the time-stepping schemes under consideration, cf. Rannacher [20] and also e.g. [6, 12, 18]. By adopting this damping procedure, we recover in each case 1–4 a stiff order of convergence equal to one for the Do scheme and equal to two for the CS scheme.

Concerning implementation, we mention that all codes have been written in Matlab, version 7.8, where all matrices have been defined as sparse. As an indication for the computing times, our implementation of the CS, MCS, HV schemes each took per time step about 0.005 cpu-sec (if $m_1 = 2m_2 = 100$) and 0.02 cpu-sec (if $m_1 = 2m_2 = 200$) on an Intel Duo Core T5500 1.6 GHz processor with 1 GB memory. For the Do scheme these times are appr. halved. Note that the times are directly proportional to the number of spatial grid points m.

3.3. Down-and-out call options. The FD discretization of the Heston PDE described in Sect. 2.2 is readily adapted to more exotic options such as barrier options. We briefly discuss here down-and-out call options. If $B \in (0, K)$ denotes the down-and-out barrier, then the spatial domain becomes $[B, S] \times [0, V]$. Next, the boundary conditions (2.3), (2.5) change to, respectively,

$$u(B, v, t) = 0 \quad (0 \leq t \leq T)$$

and
$$u(s, V, t) = (s - B)e^{-r_f t} \quad (0 \le t \le T).$$

Finally, mesh points in the s-direction are given by (2.6) with
$$\xi_i = \sinh^{-1}((B - K)/c) + i \cdot \Delta\xi \quad (0 \le i \le m_1)$$

and
$$\Delta\xi = \frac{1}{m_1} [\sinh^{-1}((S - K)/c) - \sinh^{-1}((B - K)/c)].$$

The above modifications clearly concern only a few lines in the implementation.

Lipton [14] derived a semi-analytical formula for the prices of double barrier options in the Heston model provided the correlation $\rho = 0$ and $r_d = r_f$. By using Lipton's formula with a large value for the upper barrier, the semi-discrete Heston PDE (2.12) for down-and-out barrier options has been validated in all four cases from Table 1, where we chose the barrier $B = 95 < 100 = K$ and set $\rho = 0$, $r_d = r_f = 0.03$. Moving the upper boundary for s to $S = 14K$ so as to reduce the modeling error, again an appr. second-order convergence behavior for the global spatial errors is obtained in each case, cf. Sect. 3.1.

We subsequently applied each of the ADI schemes from Sect. 3.2 together with the RKC scheme to the semi-discrete Heston PDE for down-and-out barrier options where B, S were taken as above and we considered the four original cases from Table 1. For all schemes it turned out to be advantageous, to a larger or smaller extent, to employ the damping procedure at $t = 0$ to obtain a regular behavior of the global temporal errors when the time step Δt is relatively large. The conclusions concerning the observed stability and convergence behavior of the schemes are similar to those of Sect. 3.2. In particular, we find that in all cases 1–4 the Do scheme has a stiff order of convergence equal to one and the CS, MCS, HV2 schemes possess a stiff order of convergence equal to two. Next, the global temporal errors for the latter three schemes are always close to each other in the cases 2 and 4, but in the cases 1 and 3 the HV2 scheme has somewhat larger errors than the CS, MCS schemes. Finally, for the HV1 scheme we observe again a peak in the global temporal errors in case 2. In the other three cases from Table 1 the HV1 scheme shows a stiff order of convergence equal to two.

4. Conclusions and future research

Among the schemes discussed in this paper, the MCS scheme with $\theta = \frac{1}{3}$, used with damping at $t = 0$, seems preferable for the fast, accurate and robust numerical solution of the semi-discrete Heston PDE with arbitrary correlation $\rho \in [-1, 1]$. The CS scheme with $\theta = \frac{1}{2}$ and the HV scheme with $\theta = \frac{1}{2} + \frac{1}{6}\sqrt{3}$, both applied with damping, form good alternatives. All three ADI schemes show an unconditionally stable behavior combined with a stiff order of convergence equal to two. For the CS scheme it is essential to apply damping at $t = 0$, whereas for the above HV scheme the error constant can be somewhat larger than for the MCS scheme, when damping is used. The RKC scheme as well as the HV scheme with $\theta = 1 - \frac{1}{2}\sqrt{2}$ lack robustness, as they can have an unstable behavior if the volatility-of-variance σ is close to zero. Also, the RKC scheme appears to be relatively inefficient. Finally, the Do scheme shows an unconditionally stable behavior but has only a stiff order of convergence equal to one whenever the correlation ρ is non-zero.

We conclude by mentioning some issues for future research. A main issue is a theoretical analysis of the stability and convergence properties of the ADI schemes that have been observed in the experiments, cf. Sect. 3.2. Next, a study of the

performance of ADI schemes relevant to other exotic options in the Heston model is of much interest. The use of variable time steps, especially near the initial time $t = 0$, is likely to increase the efficiency, cf. e.g. [13]. Finally, ADI schemes can be attractive in the numerical solution of other multi-dimensional PDEs from finance with mixed derivative terms, e.g. the three-dimensional hybrid Heston–Hull–White model. The extension of the ADI schemes (2.17)–(2.20) to such PDEs is straightforward. Positive results on unconditional stability of these schemes in arbitrary spatial dimensions, for pure diffusion equations with mixed derivative terms, have recently been proved in [10].

Acknowledgments

References

[1] H. Albrecher, P. Mayer, W. Schoutens & J. Tistaert, *The little Heston trap*, Wilmott Mag., January 2007, 83–92.

[2] J. Andreasen, *Back to the future*, Risk **18** (2005) 104–109.

[3] Bloomberg Quant. Finan. Devel. Group, *Barrier options pricing under the Heston model*, 2005.

[4] I. J. D. Craig & A. D. Sneyd, *An alternating-direction implicit scheme for parabolic equations with mixed derivatives*, Comp. Math. Appl. **16** (1988) 341–350.

[5] J. Douglas & H. H. Rachford, *On the numerical solution of heat conduction problems in two and three space variables*, Trans. Amer. Math. Soc. **82** (1956) 421–439.

[6] M. B. Giles & R. Carter, *Convergence analysis of Crank–Nicolson and Rannacher time-marching*, J. Comp. Finan. **9** (2006) 89–112.

[7] S. L. Heston, *A closed-form solution for options with stochastic volatility with applications to bond and currency options*, Rev. Finan. Stud. **6** (1993) 327–343.

[8] K. J. in 't Hout, *ADI schemes in the numerical solution of the Heston PDE*, in: Numerical Analysis and Applied Mathematics, eds. T. E. Simos et. al., AIP Conf. Proc. **936** (2007) 10–14.

[9] K. J. in 't Hout & B. D. Welfert, *Stability of ADI schemes applied to convection-diffusion equations with mixed derivative terms*, Appl. Num. Math. **57** (2007) 19–35.

[10] K. J. in 't Hout & B. D. Welfert, *Unconditional stability of second-order ADI schemes applied to multi-dimensional diffusion equations with mixed derivative terms*, Appl. Num. Math. **59** (2009) 677–692.

[11] W. Hundsdorfer, *Accuracy and stability of splitting with Stabilizing Corrections*, Appl. Num. Math. **42** (2002) 213–233.

[12] W. Hundsdorfer & J. G. Verwer, Numerical Solution of Time-Dependent Advection-Diffusion-Reaction Equations, Springer, Berlin, 2003.

[13] T. Kluge, *Pricing derivatives in stochastic volatility models using the finite difference method*, Dipl. thesis, TU Chemnitz, 2002.

[14] A. Lipton, Mathematical Methods for Foreign Exchange, World Scientific, Singapore, 2001.

[15] S. McKee & A. R. Mitchell, *Alternating direction methods for parabolic equations in two space dimensions with a mixed derivative*, Computer J. **13** (1970) 81–86.

[16] S. McKee, D. P. Wall & S. K. Wilson, *An alternating direction implicit scheme for parabolic equations with mixed derivative and convective terms*, J. Comp. Phys. **126** (1996) 64–76.

[17] D. W. Peaceman & H. H. Rachford, *The numerical solution of parabolic and elliptic differential equations*, J. Soc. Ind. Appl. Math. **3** (1955) 28–41.

[18] D. M. Pooley, K. R. Vetzal & P. A. Forsyth, *Convergence remedies for non-smooth payoffs in option pricing*, J. Comp. Finan. **6** (2003) 25–40.

[19] C. Randall, PDE Techniques for Pricing Derivatives with Exotic Path Dependencies or Exotic Processes, Lecture notes, Workshop CANdiensten, Amsterdam, 2002.

[20] R. Rannacher, *Finite element solution of diffusion problems with irregular data*, Numer. Math. **43** (1984) 309–327.

[21] W. Schoutens, E. Simons & J. Tistaert, *A perfect calibration ! Now what ?*, Wilmott Mag., March 2004, 66–78.

[22] S. E. Shreve, Stochastic Calculus for Finance II, Springer, New York, 2004.

[23] B. P. Sommeijer, L. F. Shampine & J. G. Verwer, *RKC: An explicit solver for parabolic PDEs*, J. Comp. Appl. Math. **88** (1997) 315–326.

[24] D. Tavella & C. Randall, Pricing Financial Instruments, Wiley, New York, 2000.

[25] J. G. Verwer, B. P. Sommeijer & W. Hundsdorfer, *RKC time-stepping for advection-diffusion-reaction problems*, J. Comp. Phys. **201** (2004) 61–79.

[26] J. G. Verwer, E. J. Spee, J. G. Blom & W. Hundsdorfer, *A second-order Rosenbrock method applied to photochemical dispersion problems*, SIAM J. Sci. Comp. **20** (1999) 1456–1480.

[27] G. Winkler, T. Apel & U. Wystup, *Valuation of options in Heston's stochastic volatility model using finite element methods*, in: Foreign Exchange Risk, eds. J. Hakala & U. Wystup, Risk Publ., 2002.

Department of Mathematics and Computer Science, University of Antwerp, Middelheimlaan 1, B-2020 Antwerp, Belgium

E-mail: karel.inthout@ua.ac.be

URL: http://win.ua.ac.be/~kihout/

KBC, Havenlaan 12, B-1080 Brussels, Belgium

E-mail: sven.foulon@kbc.be